

## Large proton contribution to the $2^+$ excitation in $^{20}\text{Mg}$ studied by intermediate energy inelastic scattering

N. Iwasa,<sup>1</sup> T. Motobayashi,<sup>2</sup> S. Bishop,<sup>2</sup> Z. Elekes,<sup>2,3</sup> J. Gibelin,<sup>4,5</sup> M. Hosoi,<sup>6</sup> K. Ieki,<sup>4</sup> K. Ishikawa,<sup>7</sup> H. Iwasaki,<sup>8</sup> S. Kawai,<sup>4</sup> S. Kubono,<sup>9</sup> K. Kurita,<sup>4</sup> M. Kurokawa,<sup>2</sup> N. Matsui,<sup>7</sup> T. Minemura,<sup>2</sup> H. Morikawa,<sup>4</sup> T. Nakamura,<sup>7</sup> M. Niikura,<sup>9</sup> M. Notani,<sup>10</sup> S. Ota,<sup>9,11</sup> A. Saito,<sup>9</sup> H. Sakurai,<sup>2</sup> S. Shimoura,<sup>9</sup> K. Sugawara,<sup>6</sup> T. Sugimoto,<sup>7</sup> H. Suzuki,<sup>8</sup> T. Suzuki,<sup>6</sup> I. Tanihata,<sup>12</sup> E. Takeshita,<sup>4</sup> T. Teranishi,<sup>13</sup> Y. Togano,<sup>4</sup> K. Yamada,<sup>2</sup> K. Yamaguchi,<sup>4</sup> and Y. Yanagisawa<sup>2</sup>

<sup>1</sup>Department of Physics, Tohoku University, Sendai, Miyagi 980-8578, Japan

<sup>2</sup>RIKEN (Institute of Physical and Chemical Research), Wako, Saitama 351-0198, Japan

<sup>3</sup>Institute of Nuclear Research of the Hungarian Academy of Sciences, P.O. Box 51, H-4001 Debrecen, Hungary

<sup>4</sup>Department of Physics, Rikkyo University, Toshima, Tokyo 171-8501, Japan

<sup>5</sup>Institut de Physique Nucléaire, IN2P3-CNRS, F-91406 Orsay, France

<sup>6</sup>Department of Physics, Saitama University, Shimo-Ohkubo, Saitama 338-8570, Japan

<sup>7</sup>Department of Physics, Tokyo Institute of Technology, Ookayama, Meguro, Tokyo 152-8551, Japan

<sup>8</sup>Department of Physics, University of Tokyo, Bunkyo, Tokyo 113-0033, Japan

<sup>9</sup>Center for Nuclear Study (CNS), University of Tokyo, RIKEN campus, Wako, Saitama 351-0198, Japan

<sup>10</sup>Physics Division, Argonne National Laboratory, Argonne, Illinois 60439, USA

<sup>11</sup>Department of Physics, Kyoto University, Kyoto 606-8502, Japan

<sup>12</sup>Research Center for Nuclear Physics, Osaka University, Ibaraki, Osaka 567-0047, Japan

<sup>13</sup>Department of Physics, Kyushu University, Hakozaki, Fukuoka 812-8581, Japan

(Received 16 June 2008; published 13 August 2008; publisher error corrected 20 August 2008)

Coulomb excitation of the proton-rich nucleus  $^{20}\text{Mg}$  was studied using a radioactive  $^{20}\text{Mg}$  beam at 58A MeV impinging on a lead target. The reduced transition probability  $B(E2; 0_{\text{g.s.}}^+ \rightarrow 2_1^+)$  was extracted to be  $177(32) e^2 \text{ fm}^4$ , which agrees with the theoretical predictions by a cluster model assuming  $^{16}\text{O} + 2p + 2p$  structure, a mean-field approach based on the angular momentum projected generator coordinate method, and the USD shell model. The ratio of the neutron-to-proton multipole matrix elements  $M_n/M_p$  in the mirror nucleus  $^{20}\text{O}$  was deduced to be 2.51(25) with the  $M_n$  value evaluated from the measured  $B(E2)$  value for  $^{20}\text{Mg}$  with the help of isospin symmetry. The results confirm the large  $M_n/M_p$  value previously reported in  $^{20}\text{O}$ , leading to the dominant role of the four valence nucleons in the  $2_1^+$  excitation and persistence of the  $^{16}\text{O}$  core in  $^{20}\text{O}$  and  $^{20}\text{Mg}$ .

DOI: 10.1103/PhysRevC.78.024306

PACS number(s): 23.20.Lv, 25.60.-t, 25.70.De

Manifestation of nuclear collectivity and shell closure in a wide range of nuclei has recently drawn much interest as seen by the recent development of exotic-beam based experiments. The  $E2$  reduced transition probability  $B(E2)$  for the  $0_{\text{g.s.}}^+ \rightarrow 2_1^+$  transition in even-even nuclei is one of the fundamental quantities that measures the degree of nuclear collectivity. Furthermore, the neutron and proton multipole matrix elements  $M_n$  and  $M_p$  have been discussed in terms of the relative importance between the neutron and proton contributions to the transition, where  $M_n(M_p)$  is defined as  $M_n(M_p) = \langle J_f || \sum_{n(p)} r_i^\lambda Y_\lambda(\Omega_i) || J_i \rangle$ . These multipole elements are especially important for neutron- or proton-rich nuclei, since their protons and neutrons can collectively behave in different ways. While  $M_p$ , which reflects the motion of protons in the nucleus, is directly related to  $B(E2)$  as  $B(E2; J_i \rightarrow J_f) = e^2 M_p^2 / (2J_i + 1)$ ,  $M_n$  for neutrons is often determined indirectly by comparing  $M_p$  with another observable, typically proton inelastic scattering result which has a sensitivity to  $M_n$ , or by comparing results obtained with different hadronic probes having different sensitivities to  $M_p$  and  $M_n$ . An alternative method uses  $B(E2)$  in the mirror nucleus. Assuming isospin symmetry,  $M_n(M_p)$  for a transition is equal to  $M_p(M_n)$  for the corresponding transition in the mirror partner.

Recently, the neutron multipole element  $M_n$  for the  $0_{\text{g.s.}}^+ \rightarrow 2_1^+$  transition in  $^{20}\text{O}$  was extracted using the proton inelastic

scattering results of Jewell *et al.* [1] and Khan *et al.* [2]. Compared with the adopted  $B(E2)$  value of  $28(2) e^2 \text{ fm}^4$  for  $^{20}\text{O}$  [3], they deduced  $|M_n|$  values of  $15(2) \text{ fm}^2$  and  $17(4) \text{ fm}^2$ , respectively, from proton inelastic scattering and the help of the Bernstein prescription [4] on the relative sensitivity. These  $M_n$  values yield the ratio of  $M_n/M_p$  of 2.9(4) and 3.25(80), respectively, suggesting dominant role of the four valence neutrons for the  $2_1^+$  excitation in  $^{20}\text{O}$ . These two results were later reanalyzed by Khoa using a compact folding model for the inelastic scattering process, and a larger  $|M_n|$  of  $22(2) \text{ fm}^2$ , which resulted in  $M_n/M_p = 4.2(3)$ , was extracted as an average [5]. This suggests the existence of systematic uncertainties in extracting the  $M_n$  value, possibly caused by insufficient knowledge on the mechanism of proton inelastic scattering; an independent determination of  $M_n$  is therefore desirable.

In the present article, we report on the first measurement of  $B(E2; 0_{\text{g.s.}}^+ \rightarrow 2_1^+)$  for  $^{20}\text{Mg}$ , the mirror nucleus of  $^{20}\text{O}$ , using intermediate-energy Coulomb excitation. As discussed above, the  $M_n$  value for  $^{20}\text{O}$  is deduced from the measured  $B(E2; 0_{\text{g.s.}}^+ \rightarrow 2_1^+)$  by assuming isospin symmetry.

The experiment was carried out using a part of the RIBF (RI Beam Factory) accelerator complex operated by RIKEN Nishina Center and Center for Nuclear Study, University of Tokyo. A radioactive  $^{20}\text{Mg}$  beam was produced by

fragmentation of a 135A MeV  $^{24}\text{Mg}$  beam, provided by the RIKEN Ring Cyclotron, bombarding a 1.35-mm-thick nickel target. The secondary beam was isotopically separated by the RIKEN projectile-fragment separator (RIPS) [6] using an aluminum energy degrader with a thickness of 691 mg/cm<sup>2</sup> and a wedge angle of 3.3 mrad placed at the dispersive focus F1. To improve the purity of  $^{20}\text{Mg}$ , an RF deflector [7] was placed around the first achromatic focus F2. The beam particles were identified event by event with the  $B\rho$ -time-of-flight (TOF)- $\Delta E$  method by using a parallel plate avalanche counter (PPAC) and a 0.3-mm-thick plastic scintillator placed, respectively, at 552 and 95 cm upstream of the final focus F3, where the secondary target was placed. By the use of the nickel target instead of the usually employed beryllium target, the number of contaminant particles was reduced and the purity of  $^{20}\text{Mg}$  was improved by a factor of 6. A further purity improvement of a factor of 3 was achieved by the RF deflector. A typical  $^{20}\text{Mg}$ -beam intensity at F3 was 0.5 kcps, which was about 9% of the total secondary-beam intensity. The major contaminant particles were  $^{16}\text{O}$ ,  $^{17}\text{F}$ , and  $^{18}\text{Ne}$  whose intensities were approximately 19%, 14%, and 20% of the secondary-beam intensity, respectively. As a secondary target, a 226-mg/cm<sup>2</sup>-thick lead plate was used to populate excited states in  $^{20}\text{Mg}$ . The average beam energy in the center of the target was 58A MeV. By way of two PPACs placed at 120 and 150 cm upstream of F3, the reaction point on the target and incident angle with respect to the beam axis were measured event by event. Their spreads at  $1\sigma$  were respectively 8 mm and 8 mrad in the horizontal direction, and 6 mm and 8 mrad in the vertical direction. Measurement with a 118-mg/cm<sup>2</sup>-thick carbon target was also performed to evaluate the contributions of nuclear excitation.

Scattered  $^{20}\text{Mg}$  were detected by an array of nine silicon telescopes arranged in a  $3 \times 3$  matrix placed 65 cm downstream from the target. Each telescope consisted of six layers of ion-implanted silicon detectors with an individual thickness of 500  $\mu\text{m}$  and an effective area of  $50 \times 50 \text{ mm}^2$ , mounted on  $56 \times 56 \text{ mm}^2$  frames. The silicon detectors in the first and second layers had 5-mm pitch strip electrodes in the vertical and horizontal directions, respectively, to measure the scattering angle. Particle identification was performed by the  $\Delta E$ - $E$  method.

Sixty-eight NaI(Tl) scintillators (DALI) [8] were placed around the target to detect deexcitation  $\gamma$ -rays from the reaction products. The detection efficiency was determined by comparison with  $^{137}\text{Cs}$ ,  $^{60}\text{Co}$ , and  $^{22}\text{Na}$  calibrated sources, and agreed with results of the Monte Carlo simulations using the GEANT3 code [9] within the uncertainty of the source activity, 3%. Based on the full-energy peak efficiency thus obtained for each detector, the total detection efficiency was obtained by considering the Doppler shift. It was, for example, 14.2% for a 1.61 MeV  $\gamma$ -ray emitted from a source moving with the velocity of  $0.34c$ . Lead shields with a thickness of 5 cm surrounded the NaI(Tl) array for background reduction. Further reduction was achieved by selecting prompt  $\gamma$ -ray emission with the NaI(Tl) timing measured relative to the beam arriving at the target. Remaining background was measured without the target in place.

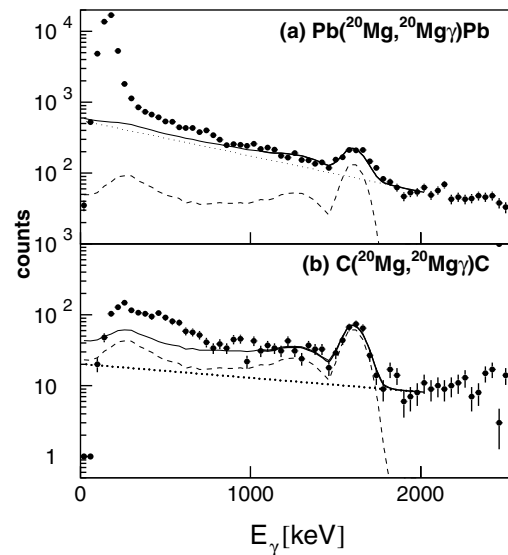


FIG. 1.  $\gamma$ -energy spectra after correcting for the Doppler shift in (a) the  $^{20}\text{Mg} + \text{Pb}$  and (b)  $^{20}\text{Mg} + \text{C}$  inelastic scattering. The solid curves represent the best fit by the simulated line shape (dashed curves) and an exponential background (dotted curves).

Figure 1 shows the energy spectra of  $\gamma$  rays measured for the lead (a) and carbon (b) targets when both the beam particle and reaction product are identified as  $^{20}\text{Mg}$ . The Doppler-shift correction is applied to obtain these spectra. A strong  $\gamma$ -line at 1.61(6) MeV is seen in the two spectra. This  $\gamma$ -line may correspond to the one at 1.598(10) MeV reported by Gade *et al.* [10] in their study of in-beam  $\gamma$ -spectroscopy following two-neutron removal from  $^{22}\text{Mg}$ . They assign the line to the  $2_1^+ \rightarrow 0_{g.s.}^+$  transition in  $^{20}\text{Mg}$ . The  $\gamma$ -line around 0.1 MeV in Fig. 1(a) may originate from the Pb target. The dashed curves in Fig. 1 show the detector response for the 1.61-MeV  $\gamma$ -rays obtained by Monte Carlo simulations using the GEANT3 code, which included intrinsic energy resolution, position, and size of the NaI(Tl) detectors, and took the Doppler effect into account. The simulated response was normalized using a  $\chi^2$  minimization procedure to best fit the observed  $\gamma$ -ray spectra. The background was assumed to be a single exponential, which probably originated from neutrons and  $\gamma$  rays from the target. As shown in Fig. 1, the experimental spectra around the 1.61 MeV peak are well reproduced by the fits.

Possible feeding from unknown higher excited states to the  $2_1^+$  state is expected only from states located below the proton-decay threshold at 2.65 MeV, 1.04 MeV above the  $2_1^+$  state, because the  $\gamma$ -decay branch of unbound states is usually extremely small. Since no  $\gamma$ -lines below 1.04 MeV are seen in the present experiment (see Fig. 1) and in the two-neutron removal experiment [10], there might be no bound excited state above 1.61 MeV, and the feeding from higher states can be ignored. This is also consistent with the energy of 3.57 MeV for the second excited state ( $4_1^+$ ) in the mirror nucleus  $^{20}\text{O}$ .

Figure 2 shows the angular distribution of the scattered  $^{20}\text{Mg}$  measured in coincidence with the 1.61 MeV  $\gamma$  rays associated with the  $^{20}\text{Mg} + \text{Pb}$  inelastic scattering. The curves represent the results of Monte Carlo simulations, where events were generated with probabilities proportional to the

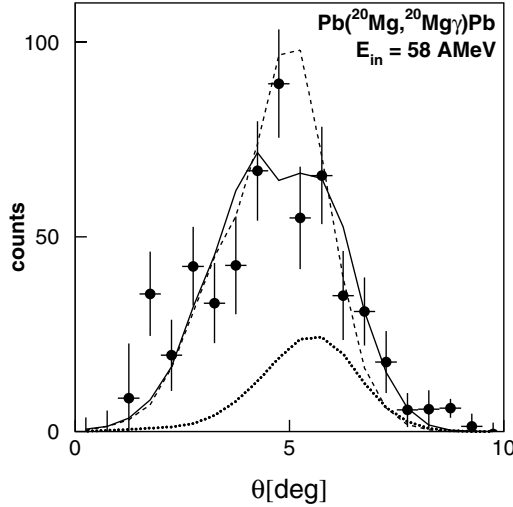


FIG. 2. Angular distribution of scattered  $^{20}\text{Mg}$  measured in coincidence with the  $\gamma$ -line at 1.61 MeV for the  $^{20}\text{Mg} + \text{Pb}$  inelastic scattering reaction. The curves represent results of Monte Carlo simulations using the optical potential parameters of  $^{17}\text{O} + ^{208}\text{Pb}$  [12]. See text.

theoretical  $\ell = 2$  angular distributions calculated using the coupled-channel code ECIS79 [11]. Three different optical-potential parameter sets, which were determined from the elastic-scattering data of  $^{17}\text{O} + ^{208}\text{Pb}$  at  $E_{\text{lab}} = 84\text{A MeV}$  [12],  $^{20}\text{Ne} + ^{208}\text{Pb}$  at  $E_{\text{lab}} = 40\text{A MeV}$  [13], and  $^{40}\text{Ar} + ^{208}\text{Pb}$  at  $E_{\text{lab}} = 41\text{A MeV}$  [14], were employed, while only the result with the  $^{17}\text{O} + ^{208}\text{Pb}$  potential is shown in the figure. In the calculation, the Coulomb- and nuclear-deformation parameters,  $\beta_2^{\text{C}}$  and  $\beta_2^{\text{N}}$ , are involved as the coupling strength. The former is related to  $B(E2; 0_{\text{g.s.}}^+ \rightarrow 2_1^+)$  as  $\beta_2^{\text{C}} = 4\pi\sqrt{B(E2; 0_{\text{g.s.}}^+ \rightarrow 2_1^+)}/3ZeR^2$ , and  $\beta_2^{\text{N}}$  measures the nuclear excitation strength. The dashed and dotted curves in Fig. 2 correspond, respectively, to the Coulomb and nuclear components with  $\beta_2^{\text{C}}$  and  $\beta_2^{\text{N}}$  obtained by a procedure to be described later. The theoretical curves are obtained by taking into account the response of the detection system simulated by Monte Carlo simulations which will also be described later. As seen in the figure, the experimental angular distribution is well reproduced by the calculation assuming an angular momentum transfer  $\ell = 2$ . This puts on firmer ground the  $2^+$  assignment to the 1.6 MeV state proposed by Gade *et al.* [10].

To extract the  $B(E2; 0_{\text{g.s.}}^+ \rightarrow 2_1^+)$  value, the nuclear excitation component should be evaluated together with the dominant Coulomb-excitation amplitude, which is responsible for  $B(E2)$  in the  $^{20}\text{Mg} + \text{Pb}$  inelastic scattering. The analysis was made using two independent procedures. The first one is to use  $\beta_2^{\text{C}}$  or  $B(E2)$  from the mirror nucleus  $^{20}\text{O}$ . As discussed earlier, the neutron multipole matrix element  $M_n$  is extracted from  $B(E2)$  for the mirror nucleus if isospin symmetry is assumed. The nuclear deformation parameter  $\beta_2^{\text{N}}$ , which is used to calculate the nuclear excitation contribution, can be related to the  $M_n$  and  $M_p$  values with the help of the Bernstein prescription [4] as follows. The ratio of the nuclear deformation length  $\delta_F = \beta_2^{\text{N}}R$  for the experimental probe  $F$

to the Coulomb one  $\delta_p = \beta_2^{\text{C}}R$  is given by

$$\frac{\delta_F}{\delta_p} = \frac{1 + (b_n^F/b_p^F)(M_n/M_p)}{1 + (b_n^F/b_p^F)(N/Z)}, \quad (1)$$

where  $b_{n(p)}^F$  is the interaction strengths of the probe  $F$  with neutrons (protons) in the nucleus. For the nuclear excitation in  $^{20}\text{Mg} + \text{Pb}$  inelastic scattering, the ratio  $b_n^F/b_p^F$  could be evaluated as  $b_{n(p)}^F = Z_F b_{n(p)}^p + N_F b_{n(p)}^n$ , where  $Z_F$  and  $N_F$  are the proton and neutron numbers of the probe  $F$  (Pb). By using  $b_n^p/b_p^p = b_n^n/b_p^n = 3$  for proton and neutron scattering around the present energy [4],  $b_n^F/b_p^F$  was estimated to be 0.81 for Pb. Neutron deformation  $\beta_2^{\text{N}}$  is related to  $\beta_2^{\text{C}}$  by Eq. (1), since  $M_n$  is given from the known  $M_p$  value for  $^{20}\text{O}$  and  $|M_p|$  is obtained from  $\beta_2^{\text{C}}$ . Thus,  $|M_p|$  is determined by adjusting the  $\beta_2^{\text{C}}$  or  $B(E2)$  value to reproduce the experimental cross section [15].

The second method to evaluate the nuclear excitation effect is to use the  $^{20}\text{Mg} + \text{C}$  inelastic-scattering data. Since the contribution of the Coulomb excitation is negligibly small, the  $\beta_2^{\text{N}}$  value can be determined by reproducing the experimental cross section of  $^{20}\text{Mg} + \text{C}$  inelastic scattering.

To compare the experimental and calculated yield, the detection response was evaluated by Monte Carlo simulations using the code GEANT3 as mentioned. The beam size and angular spread of the beam at the target, and the finite angular acceptance of the silicon telescopes were taken into account. The latter yields the detection efficiencies of 67(1)% and 81(3)%, for  $^{20}\text{Mg} + \text{Pb}$  and  $^{20}\text{Mg} + \text{C}$ , respectively. The quoted errors stem from the choice of optical potential.

The experimental cross sections of the  $^{20}\text{Mg} + \text{Pb}$  and  $^{20}\text{Mg} + \text{C}$  inelastic scatterings were deduced from the  $\gamma$ -ray yields to be 105(10) and 20(2) mb, respectively. The quoted errors are dominated by the statistical uncertainties associated with the fit, while the systematic errors, which are mainly due to the uncertainties in the  $\gamma$ -ray efficiency calculations (3%) and the error in the detection efficiency for scattered particles, are added in quadrature. By employing the first procedure for evaluation of the nuclear excitation contribution,  $\beta_2^{\text{C}}$  was deduced to be 0.48(2), 0.41(2), and 0.43(2) using the  $^{17}\text{O} + ^{208}\text{Pb}$ ,  $^{20}\text{Ne} + ^{208}\text{Pb}$ , and  $^{40}\text{Ar} + ^{208}\text{Pb}$  potential parameters, respectively. With the second procedure, the resultant  $\beta_2^{\text{C}}$  values were 0.46(3), 0.47(3) and 0.47(3), respectively, for the three optical potentials. Since the second method is expected to be less reliable due to the expected uncertainties regarding the use of the same  $\beta_2^{\text{N}}$  value for the carbon and lead targets and the large potential dependence in  $^{20}\text{Mg} + \text{C}$  analysis, the results are used only to evaluate the error. By taking an average of the three values deduced with the Bernstein prescription, we determined  $\beta_2^{\text{C}}$  to be 0.44(4); the error evaluated by taking the maximum deviation of the above  $\beta_2^{\text{C}}$  values. The corresponding  $B(E2; 0_{\text{g.s.}}^+ \rightarrow 2_1^+)$  value for  $^{20}\text{Mg}$  is  $177(32) e^2 \text{fm}^4$  or  $|M_p|$  of  $13.3(12) \text{fm}^2$ .

The extracted  $|M_p|$  value for  $^{20}\text{Mg}$  leads to the same value of the neutron multipole matrix element  $|M_n|$  for  $^{20}\text{O}$  based on isospin symmetry as discussed earlier. The value  $13.3(12) \text{fm}^2$  is slightly smaller than but agrees within the errors with  $15(2) \text{fm}^2$  and  $17(4) \text{fm}^2$  reported by Jewell *et al.* [1] and Khan *et al.* [2], who applied the Bernstein prescription to extract the



multipole elements from the proton inelastic-scattering data. It should be noted that the error is smaller for the present result obtained by using the mirror  $B(E2)$ . On the other hand, the  $|M_n|$  value of 22(2) fm<sup>2</sup> extracted by Khoa [5] using the compact folding model is inconsistently larger. From the present experimental data, the  $M_p/M_n$  value in <sup>20</sup>Mg or the  $M_n/M_p$  value in <sup>20</sup>O was extracted to be 2.51(25) by using the known  $|M_p|$  value for <sup>20</sup>O. It is again consistent with the two earlier results of 2.9(4) and 3.25(80) by Jewell *et al.* [1] and Khan *et al.* [2], respectively, but smaller than 4.2(3) by Khoa [5]. The present result confirms qualitatively the larger  $M_n$  value for the  $0^+-2^+$  transition in <sup>20</sup>O compared with  $M_p$  reported in the earlier studies. For a more detailed discussion, the disagreement with the Khoa's results with a microscopic analysis needs to be understood. Systematical uncertainties in analyzing the reaction process, and possible isospin violation in the transition, and so on, should be carefully examined.

There are a few theoretical studies on the nuclear structure of <sup>20</sup>O and <sup>20</sup>Mg. Descouvemont performed a three-body cluster model calculation, assuming the <sup>16</sup>O + 2p + 2p configuration for <sup>20</sup>Mg, with the generator coordinate method (GCM) [17]. The extracted  $B(E2)$  values were 209 e<sup>2</sup> fm<sup>4</sup> and 148 e<sup>2</sup> fm<sup>4</sup> with the Volkov V2 [18] and Minnesota [19] forces, respectively. Rodriguez-Guzman *et al.* calculated  $B(E2)$  by a mean-field approach using the angular momentum-projected generator coordinate method (AMPGCM), to be 180 e<sup>2</sup> fm<sup>4</sup> [20]. These results agree with the value 177(32) e<sup>2</sup> fm<sup>4</sup> obtained in the present study. They are also consistent with the corresponding  $|M_n|$  values for the mirror nucleus <sup>20</sup>O reported by Jewell *et al.* [1] and Khan *et al.* [2], but smaller than the one by Khoa [5]. Shell-model calculations for  $B(E2)$  were also carried out with the USDA and USDB effective interaction [21] using the code OXBASH [22]. By using effective charges of  $e_p = 1.3e$  and  $e_n = 0.5e$ , the results 165e<sup>2</sup> fm<sup>4</sup> and 172e<sup>2</sup> fm<sup>4</sup>, respectively, were obtained for <sup>20</sup>Mg, which again agree with the  $B(E2)$  value extracted in the present experimental study.

The  $M_n/M_p$  ( $M_p/M_n$ ) value of 2.51(25) for <sup>20</sup>O (<sup>20</sup>Mg) is considerably larger than the "collective" limit,  $N/Z = 1.5$ , suggesting a dominant role of the valence neutrons (protons). The extracted  $M_n/M_p$  value can be understood with a simple picture where the <sup>16</sup>O core is inert and only the four valence nucleons are responsible for the  $2^+$  excitation. If the effects beyond the particle-hole excitation in the active shells are accounted for by the effective charges, the  $M_n/M_p$  ( $M_p/M_n$ ) ratio for <sup>20</sup>O (<sup>20</sup>Mg) should be equal to  $e_p/e_n$  as in the above shell model calculations, resulting in the ratio of 2.6 which is in excellent agreement with the present result of 2.51(25) in the case of using standard values  $e_p = 1.3e$  and  $e_n = 0.5e$ .

This leads to a picture that the shell closure persists in the mirror pair <sup>20</sup>O and <sup>20</sup>Mg. It should be noted that further reduction of the effective charge, which was reported recently in the neutron-rich nuclei <sup>15</sup>B and <sup>17</sup>B [23–25] and might be necessary to reproduce low  $B(E2)$  values reported for the  $0^+-2^+$  transition in <sup>16</sup>C [26,27], is not necessary in this case. This conclusion is consistent with the mean-field calculations by Rodriguez-Guzman *et al.* [20], where the potential energy surface exhibits a deep minimum in the spherical shape in contrast to heavier magnesium isotopes.

To summarize, we have measured the reduced transition probability  $B(E2; 0_{g.s.}^+ \rightarrow 2_1^+)$  for <sup>20</sup>Mg by studying intermediate-energy inelastic scattering of <sup>20</sup>Mg with lead and carbon targets in inverse kinematics. The measured energy 1.61(6) MeV of the deexcitation  $\gamma$ -rays is consistent with 1.598(10) MeV determined in a two-neutron removal study [10]. The angular distribution is consistent with the angular momentum transfer  $\ell = 2$ , confirming the  $2^+$  assignment to the 1.6 MeV state in the same study. The extracted  $B(E2; 0_{g.s.}^+ \rightarrow 2_1^+)$  value is consistent with the theoretical predictions with the three-body cluster model by Descouvemont [17], the mean-field calculations by Rodriguez-Guzman *et al.* [20], and the USD shell model. The ratio  $M_n/M_p$  for the mirror nucleus <sup>20</sup>O was obtained by evaluating  $M_n$  from the measured  $B(E2)$  value assuming isospin symmetry in the mirror transitions. The extracted large ratio of 2.51(25) is essentially consistent with the earlier results obtained by coupling proton inelastic scattering data with the known  $B(E2)$  value for <sup>20</sup>O, and indicates that valence nucleons play the major role in the excitation. The  $M_n/M_p$  ratio is close to the ratio of standard effective charges,  $e_p/e_n$ , suggesting the persistence of the  $N = Z = 8$  shell closure in <sup>20</sup>O and <sup>20</sup>Mg. However, there remains some disagreement among the  $M_n/M_p$  ratios extracted from different experiments with different methods; particularly, the result obtained by analyzing the inelastic scattering data with a folding model [5] is inconsistent with other experimental results including the present one. Further investigation on the reaction mechanism is desirable for more quantitative understanding of the nuclear structure of <sup>20</sup>O and <sup>20</sup>Mg, and for discussion on possible isospin violation effects.

## ACKNOWLEDGMENTS

We would like to thank the staff of the RIKEN Nishina Center for their help during the experiment. The present work was partly supported by the Grant-in-Aid for Young Scientists of the Japan Ministry of Education, Science, Sports, and Culture under the program no. (B)14740149.

- [1] J. K. Jewell *et al.*, Phys. Lett. **B454**, 181 (1999).
- [2] E. Khan *et al.*, Phys. Lett. **B490**, 45 (2000).
- [3] S. Raman, C. W. Nestor, Jr., and P. Tikkanen, At. Data Nucl. Data Tables **78**,1 (2001).
- [4] A. M. Bernstein *et al.*, Phys. Lett. **B103**, 255 (1981).
- [5] D. T. Khoa, Phys. Rev. C **68**, 011601(R) (2003).
- [6] T. Kubo *et al.*, Nucl. Instrum. Methods Phys. Res. B **70**, 309 (1992).

- [7] K. Yamada, T. Motobayashi, and I. Tanihata, Nucl. Phys. **A746**, 156c (2004).
- [8] T. Motobayashi *et al.*, Phys. Lett. **B346**, 9 (1995).
- [9] Detector description and simulation tool by the CERN, Geneva, Switzerland.
- [10] A. Gade *et al.*, Phys. Rev. C **76**, 024317 (2007).
- [11] J. Raynal, coupled channel code ECIS79, unpublished.
- [12] J. Barrette *et al.*, Phys. Lett. **B209**, 182 (1988).

- [13] T. Suomijärvi *et al.*, Nucl. Phys. **A491**, 314 (1989).
- [14] T. Suomijärvi *et al.*, Nucl. Phys. **A509**, 369 (1990).
- [15] There are two possibilities for the absolute sign of  $M_n$  and  $M_p$ . We assumed that the ratio of  $M_n/M_p$  is positive. If it is negative, the isovector  $E2$  matrix element  $B(E2_{IV}) = (1/4)(M_n - M_p)^2$  introduced by Endt [16] exceeds the recommended upper limit.
- [16] P. M. Endt, At. Data Nucl. Data Tables **55**, 171 (1993).
- [17] P. Descouvemont, Phys. Lett. **B437**, 7 (1998).
- [18] A. B. Volkov, Nucl. Phys. **74**, 33 (1965).
- [19] D. R. Thompson, M. LeMere, and Y. C. Tang, Nucl. Phys. **A286**, 53 (1977).
- [20] R. Rodriguez-Guzman, J. L. Egido, and L. M. Robledo, Nucl. Phys. **A709**, 201 (2002).
- [21] B. A. Brown and W. A. Richter, Phys. Rev. C **74**, 034315 (2006).
- [22] B. A. Brown, shell model code OXBASH, MSU-NSCL report 524 (1988).
- [23] H. Ogawa *et al.*, Phys. Rev. C **67**, 064308 (2003).
- [24] Zs. Dombrádi *et al.*, Phys. Lett. **B621**, 81 (2005).
- [25] Y. Kondo *et al.*, Phys. Rev. C **71**, 044611 (2005).
- [26] N. Imai *et al.*, Phys. Rev. Lett. **92**, 062501 (2004).
- [27] H. J. Ong *et al.* (to be published).